Bioinformatics analysis of KLF2 as a potential prognostic factor in ccRCC and association with epithelial-mesenchymal transition

FANGFANG HU[1,2*], YAN REN[3*], ZUNYUN WANG[2,3], HUI ZHOU[1,2], YUMEI LUO[2], MINGHUA WANG[2], FAQING TIAN[2], JIAN ZHENG[2], JUAN DU[1,2] and GANG PANG[3]

[1]Department of Physiology, School of Basic Medical Sciences, Anhui Medical University, Hefei, Anhui 230032;
[2]The Second Affiliated Hospital, School of Medicine, The Chinese University of Hong Kong, Shenzhen,
Guangdong 518172; [3]Department of Human Anatomy, School of Basic Medical Sciences,
Anhui Medical University, Hefei, Anhui 230032, P.R. China

Abstract. Clear cell renal cell carcinoma (ccRCC) is a primary pathological subtype of RCC and has poor clinical outcome. Krüppel-like factors (KLFs), which are zinc-finger proteins, may be involved in ccRCC development and progression. KLFs belong to the zinc-finger family of DNA-binding transcription factors and regulate transcription of downstream target genes. KLFs are involved in cancer development. The present study aimed to investigate the role of KLFs in ccRCC prognosis. The Cancer Genome Atlas database and multifactorial analysis showed that KLFs were widely expressed in pan-cancers and KLF2 was an independent protective factor for ccRCC prognosis. Patients with low KLF2 expression had a low survival probability and expression of KLF2 was downregulated in patients with ccRCC with high pathological grade (II + III vs. I). In addition, western blot and reverse transcription-quantitative PCR revealed that KLF2 was expressed at low levels in ccRCC cell lines and overexpression of KLF2 inhibited cell migration. In addition, KLF2 expression was negatively correlated with methylation. KLF2 expression was elevated following treatment of ccRCC cells with DNA methyltransferase inhibitor. A prognostic risk index prediction model was constructed based on multiple Cox regression. The receiver operating characteristic curve was 0.780 (area under curve >0.5). Furthermore, Gene Ontology enrichment analysis showed that 'cell adhesion' and 'junction' were negatively correlated with KLF2 and that high-risk group exhibited significantly activated 'epithelial-mesenchymal transition'. Western blot analysis showed that overexpression of KLF2 increased expression of E-cadherin, while decreasing levels of N-cadherin and vimentin. The present study highlighted the role of KLFs in ccRCC prognosis prediction and provides a research base for the search of validated prognostic biological markers for ccRCC.

Introduction

Clear cell renal cell carcinoma (ccRCC) is a primary subtype of RCC. Approximately 80% of patients with RCC are diagnosed with ccRCC, with males exhibiting a higher incidence of ccRCC than females (1-3). Early detection of ccRCC is difficult due to its insidious occurrence and lack of reliable biomarkers; thus, the majority of patients are diagnosed during the late stages of the disease (4,5). In addition, ccRCC is insensitive to traditional chemoradiotherapy (6-8). Moreover, even following surgical treatment, there are high rates of metastasis and recurrence (9-11). The outcome of surgical treatment is closely related to the clinical stage, with survival rates of 81% for stage I, 74% for stage II, 53% for stage III and 8% for stage IV (12). Therefore, identifying biomarkers for ccRCC is key for early diagnosis and improving prognosis.

Krüppel-like factors (KLFs) belong to a family of transcription factors that have a Cys2-His2 zinc-finger domain at the C-terminal region, which binds to GC and CGGA-boxes of DNA. At the N-terminal region, KLFs have a transcription regulatory motif that binds to transcription-activation or repressive factors (13-15). The first KLF (KLF1) was identified in mammalian red blood cells in 1993 (16). Following identification of KLF1 and KLF17, a number of KLF genes were found in the human genome (17). These KLF proteins are expressed in a variety of human tissue and exhibit diverse functions in physiological processes such as maintenance of internal environmental homeostasis, immune response, inflammation, neurogenesis and organ development (18-25). Genome-wide

Correspondence to: Dr Juan Du, The Second Affiliated Hospital, School of Medicine, The Chinese University of Hong Kong, 53 Aixin Road, Longgang, Shenzhen, Guangdong 518172, P.R. China
E-mail: dujuan@cuhk.edu.cn

Dr Gang Pang, Department of Human Anatomy, School of Basic Medical Sciences, Anhui Medical University, 81 Meishan Road, Hefei, Anhui 230032, P.R. China
E-mail: panggang@ahmu.edu.cn

*Contributed equally

knockout of KLF family members leads to developmental abnormality and mortality. For example, *klf15$^{-/-}$* mice have enlarged hearts (26), *klf6$^{-/-}$* or *klf1$^{-/-}$* mice have abnormal hematopoietic system (27,28). *klf2$^{-/-}$* or *klf5$^{-/-}$* mice die in utero during embryonic life (29,30). Previous studies have revealed that KLFs participate in proliferation, apoptosis, epithelial-mesenchymal transition (EMT), angiogenesis and other malignant biological behavior of cancer (14,31-33). KLF4 inhibits EMT and proliferation of endometrial cancer cells, whilst KLF8 promotes EMT and proliferation of bladder cancer cells (34,35); these findings suggest that the KLF gene family may serve a critical role in cancer genesis and prognosis.

The present study systematically analyzed expression and clinical application of KLF genes in ccRCC. KLF gene expression levels and their association with clinical prognosis of ccRCC were analyzed using public databases and findings were validated using *in vitro* cellular assays.

Materials and methods

The cancer genome atlas (TCGA) database. The clinical data and gene expression of patients with ccRCC were obtained from TCGA database (portal.gdc.cancer.gov; data collected June 2021). Using the archive of the TCGA Kidney Renal Clear Cell Carcinoma (KIRC) project (portal.gdc.cancer.gov; data collected June 2021), transcriptome maps of KLFs were extracted to obtain gene transcription information. Demographic and clinical characteristics, including age, tumor grade and stage at diagnosis (TNM classification), were obtained from the electronic records.

DNA methylation and genetic alteration. CBioPortal Cancer Genomics (cbioportal.org; data collected June 2021) is an open resource web platform that integrates multiple cancer genome databases, such as TCGA and the International Cancer Genome Consortium. Using cBioPortal, KLF2 and KLF11 mutations were analyzed in TCGA ccRCC cohort (portal.gdc.cancer.gov; data collected June 2021). This tool provides real-time access and visualization of DNA methylation profiles and gene expression from TCGA. The methylation level of promoter region of KLF2 was retrieved from MethHC (bioinfo-zs.com/smartapp/). Significant methylation sites were selected as candidate sites according to P<0.05 based on results from univariate Cox regression analysis. The correlation between two factors was evaluated by the Pearson's correlation test.

Biological pathway enrichment analysis. Gene Ontology and Kyoto Encyclopedia of Genes and Genomes pathway enrichment analysis was conducted using Metascape 3.5 (metascape.org). Gene set variation analysis (GSVA) was also used to assess the variations in pathway enrichment among patients with high and low risk score) via the 'GSVA' R package. A total of 50 hallmark gene sets were obtained from the Molecular Signatures Database (MSigDB; gsea-msigdb.org/gsea/msigdb/). Analysis of the intersection of low level of KLF2 and KLF11 activated genes using Venn diagram.

Cell culture. The human ccRCC cell lines 769-P, 786-O and OR-SC-2 and HK-2, 293(T) (normal renal tubular epithelial cell line) were obtained from the Affiliated Hospital of Yangzhou University (Suzhou, China). 293(T) cells were cultured in DMEM (Biological Industries) and other cells were cultured in RPMI 1640 medium (Biological Industries), supplemented with 10% fetal bovine serum (VivaCell Biosciences, Ltd.) and 1% penicillin/streptomycin solution (cat. no. C0222; Beyotime Institute of Biotechnology). The cell culture was maintained at 37°C and 5% CO_2. Cells were treated with 5-aza-2'-deoxycytidine 5 μM (5-AZA-CdR; cat. no. HY-A0004; MedChemExpress) for 24 h in a cell incubator at 37°C with 5% CO_2.

Lentivirus transduction and cell transfection. For KLF2 overexpression plasmid (human cDNA was cloned and inserted into a pCDH-CMV-MCS-EF1-copGFP-T2A-Puro) and 2nd packaging plasmids psPAX2, pMD2.G from GENERAL BIOL. The psPAX2 (12 μg) packaging and pMD2.G (9 μg) envelope plasmids were co-transfected with pCDH-KLF2 (4 μg). The plasmid ratio was pCDH-KLF2: psPAX2: pMD2.G=4:3:1. Subsequently, the overexpression plasmid of KLF2 and control plasmid were transfected into 293(T) cells using Lipofectamine$^®$ 3000 (Invitrogen; Thermo Fisher Scientific, Inc.) in a 100-mm dish (5x10^6 cells) and maintained in an incubator at 37°C with 5% CO_2. The medium was replaced with fresh medium after 6 h. Following incubation for 48 h, the viral supernatant was harvested at 4°C for 5 min at 2,000 g, immediate added to 786-O and 769-P cells and incubated with 8 μg/ml polybrene (cat. no. C0351; Beyotime Institute of Biotechnology). The multiplicity of infection (MOI) infected cells was 10. Stably transfected cells were selected with 2.5 μg/ml puromycin (cat. no. ST551; Beyotime Institute of Biotechnology) for three days following 48 h viral infection. Cells were cultured in RPMI 1640 medium containing 1% penicillin/streptomycin solution, while 2.5 μg/ml puromycin was added for maintenance.

Reverse transcription-quantitative (RT-q) PCR. According to the manufacturer's protocol, total cell RNA in six-well cell culture plates was isolated using TRIzol$^®$ reagent (cat. no. 10296028; Invitrogen; Thermo Fisher Scientific, Inc.). Each well contained ~2x10^5 cells. Subsequently, total RNA (1 μg) was reverse transcribed into cDNA using NovoScript$^®$ Plus All-in-one 1st Stand cDNA Synthesis SuperMix (gRNA Purge; cat. no. E047-01A; Suzhou Novoprotein Technology, Ltd.) according to the manufacturer's protocol. NovoStart$^®$ SYBR Green Color qPCR SuperMix kit (cat. no. E168-01B; Suzhou Novoprotein Technology, Ltd.) was used for amplification. Thermocycling conditions were as follows: 95°C for 30 sec, followed by 40 cycles of 95°C for 5 sec and 60°C for 30 sec. The expression of genes was normalized to that of GAPDH, which was used as an endogenous control. The $2^{-\Delta\Delta Cq}$ method (36) was performed to analyze mRNA expression levels. The primers are shown in Table I.

Western blotting. Cells were washed three times with cold PBS. Total protein was extracted using RIPA lysis buffer (cat. no. P00013B; Beyotime Institute of Biotechnology) and the protein concentration was measured by BCA (cat. no. P0009; Beyotime Institute of Biotechnology). Then, the protein was separated by 10% SDS-PAGE (20 μg per well and transferred onto a PVDF membrane. Subsequently, the membrane was
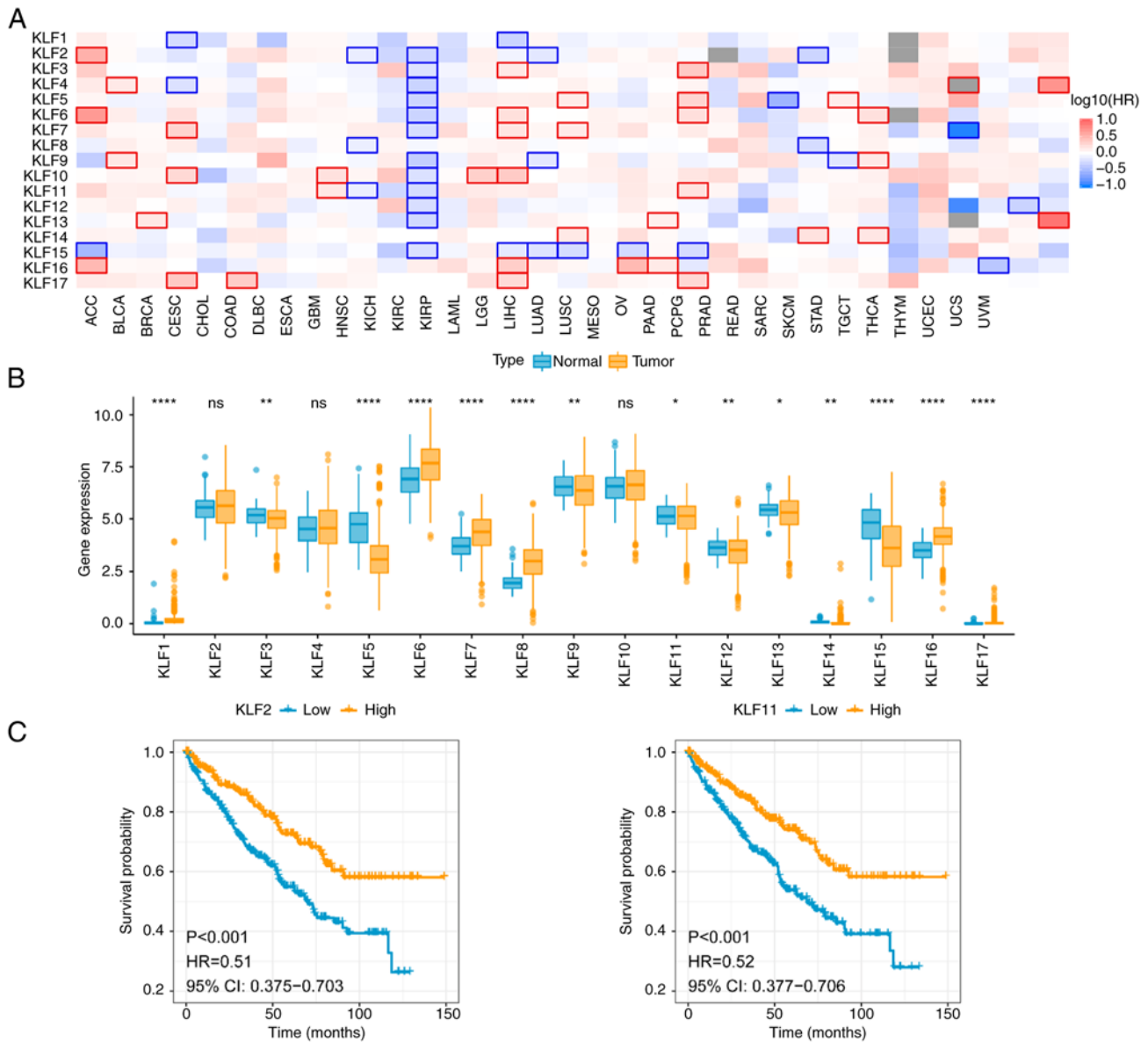
Figure 1. Expression of KLFs in pan-cancers and association with prognosis of patients with ccRCC. (A) KLFs mRNA expression in ccRCC and pan-cancers in The Cancer Genome Atlas dataset. (B) mRNA levels of KLFs in ccRCC (yellow) and normal (blue) tissue. *P<0.05, **P<0.001 and ****P<0.0001 vs. normal. (C) Kaplan-Meier curves for survival associated with KLF2 and KLF11 expression. KLF, Krüppel-like factor; ccRCC, clear cell renal cell carcinoma; ns, not significant.

Table I. Primers for reverse-transcription quantitative PCR assay.

Gene	Primer sequence (5'-3')
KLF2-Forward	CACCAAGAGTTCGCATCTGA
KLF2-Reverse	CGTGTGCTTTCGGTAGTGG
GAPDH-Forward	GGGGTCATTGATGGCAACAATA
GAPDH-Reverse	ATGGGGAAGGTGAAGGTCG

KLF, Krüppel-like factor.

blocked with 5% milk at room temperature for 1 h and incubated with primary antibodies against KLF2 (1:1,000; cat. no. 340341; Zen-Bio, Inc.), GAPDH (1:1,000; cat. no. R24404; Zen-Bio, Inc.), E-cadherin (1:1,000; cat. no. 340341; Zen-Bio, Inc.), N-cadherin (1:1,000; cat. no. 380671; Zen-Bio, Inc.) and vimentin (1:1,000; cat. no. 380771; Zen-Bio, Inc.) at 4˚C overnight. The membrane was washed and incubated with horseradish peroxidase-labelled secondary antibody (cat. no. #S001; 1:5,000; Affinity Biosciences, Ltd.) for 2 h at room temperature. The membrane was washed three times with PBS-0.1% Tween-20 for 5 min each. A chemiluminescent substrate kit (cat. no. BL520A; Biosharp Life Sciences) and iBright CL1000 imaging system (Invitrogen; Thermo Fisher Scientific, Inc.) were used to detect the proteins. Each set of experiments was repeated at least three times, with GAPDH as the internal reference control, and the relative amounts of protein bands were analyzed using ImageJ software (Version 1.48; National Institutes of Health).

Wound healing assay. To analyze cell migration, normal and KLF2 overexpressing 786-O and 769-P cells were seeded in a 6-well plate at a concentration of $1x10^5$ cells/well with 80% confluency. Using the tip of a 10-μl sterile pipette, a wound was scratched throughout the center of the well. Next, wells were gently rinsed twice with PBS to remove isolated cells and residual serum. Subsequently, all wells were refilled with fresh serum-free RPMI-1640 (Biological Industries) and cells were cultured for 24 and 48 h at 37°C and 5% CO_2. Photographs of cell migration were taken at 24 and 48 h after injury by using an inverted fluorescence microscope (MF53-N; Guangzhou Micro-short Technology Co., Ltd.) with bright field at x40 magnification. The wound area was calculated using ImageJ 1.48v (National Institutes of Health) and migration rates were calculated from area ratios. Mobility was calculated as follows: Mobility rate=(area of the starting scratch-area of the current scratch)/area of the starting scratch x100, and the result was used to determine the migration capacity of the cells.

Tissue microarray (TMA) and immunohistochemistry (IHC). A total of 20 tissue samples from patients with ccRCC were obtained from The Second Affiliated Hospital, School of Medicine, The Chinese University of Hong Kong, and a waiver of informed consent was granted by the hospital ethics committee. Tissue was fixed in 4% paraformaldehyde for 2-3 days, dehydrated, embedded in paraffin and cut into 4 μm thick sections. TMAs were dewaxed and rehydrated. Sections were placed sequentially in xylene I for 15 min-xylene II for 15 min-xylene III for 15 min-anhydrous ethanol I for 5 min-anhydrous ethanol II for 5 min-85% alcohol for 5 min-75% alcohol for 5 min-distilled water wash. Antigen repair was performed using EDTA (pH 9.0) by heating at 100°C in a microwave oven for 8 min to boiling, ceasing for 8 min and then for 7 min. 3% H_2O_2 to block endogenous peroxidase activity then incubating with 2% BSA (cat. no. G5001; Wuhan Servicebio Technology Go, Ltd.) for 30 min at room temperature. Finally, anti-KLF2 (1:100; cat. no. #DF13602; Affinity Biosciences, Ltd.) was incubated overnight at 4°C. The sections were incubated for 50 min at room temperature with horseradish peroxidase-conjugated secondary antibody (1:200; cat. no. GB23303; Wuhan Servicebio Technology Co., Ltd.). Tissue specimens were subsequently stained with 1X 3,3'-diaminobenzidine (cat. no. ZLI-9018; Beijing, ZSGB-BIO Technology Co, Ltd.) for 2 min under the inverted fluorescence microscope (Zesiss Aixo Vert. A1; Carl Zeiss AG) with bright field, then washed with PBS. Images obtained under a Nikon E100 microscope NIKON DS-U3 system scan. CaseViewer 2.4 (3DHistech, Ltd.) software was observed and intercepted at x10 and x40 magnification, respectively.

As previously described, H-score was determined based on the number and staining intensity of positive cells (37,38). Briefly, H-score was calculated as follows: (% weak intensity cells x 1) + (% moderate intensity cells x 2) + (% strong intensity cells x 3). The image scanning software AIpathwell (v1.0, Wuhan Servicebio Technology Co, Ltd.) analyses and calculates the H-score according. The intensity of positive cells was graded as 0 (negative, unstained), 1 (weak), 2 (moderate) and 3 (strong).

Statistical analysis. The gene expression values were converted into a non-overlapping number of exon fragments per kilobase to attain the normalized expression of KLFs. Survival analysis was evaluated using the R package 'survival' (Version:3.2-11, cran.r-project.org/web/packages/survival/index.html). The survival rates of patients in different test groups were analyzed using Kaplan Meier (K-M) curve. The final prognostic K-M plots were constructed using a log-rank P-value, 95% confidence interval (CI) and hazard ratio (HR). For recurrence-free survival with HR and 95% CI, univariate and multivariate Cox proportional risk regression analysis was performed for KLFs and clinical characteristics. The risk score formula was as follows: Risk score=0.025587 x age + [0.406461 x (Grade 3 + Grade 4)] + [1.088888 x (Stage III + Stage IV)] + [-0.2134 x KLF2] + [-0.197943 x KLF11]. The K-M curve showed two sets of survival states; receiver operating characteristics (ROC) curve assesses the predictive value of the prediction. P<0.05 was considered to indicate a statistically significant difference. The statistical analysis of *in vitro* expression results was performed using paired Student's t-test and one-way ANOVA followed by post hoc Tukey's test with GraphPad Prism 8.0.2 (GraphPad Software, Inc.). Data are presented as mean ± SD from at least three independent experiments.

Results

Exploration of KLFs and ccRCC prognosis. To investigate the association between KLFs and clinical prognosis of ccRCC, KLF mRNA expression in TCGA database was analyzed. KLFs were downregulated in ccRCC tissue (Fig. 1A). By contrast, data from TCGA database indicated that KLFs were expressed in numerous types of human cancer, such as adrenocortical carcinoma and uterine corpus endometrial carcinoma. These findings suggested that KLFs may serve an inhibitory role in progression of urological tumor. The mRNA levels of 17 KLFs in ccRCC and normal tissue were examined in the TCGA-KIRC database. The mRNA expression profiles of KLFs indicated that the majority of KLFs were downregulated in ccRCC compared with in normal tissue, including KLF3, KLF5, KLF9, KLF11, KLF12, KLF13, KLF14 and KLF15 (Fig. 1B). By contrast, KLF1, KLF6, KLF7, KLF8, KLF16 and KLF17 were highly expressed in tumor tissue. KLF2, KLF4 and KLF10 showed no significant difference between normal and tumor tissue. Collectively these data suggest a role for KLFs in ccRCC progression.

Univariate and multivariate Cox analysis of KLFs and clinical prognosis. To evaluate the prognostic value of the expression of KLFs, univariate Cox regression analysis was performed (Table II). Age, grade, stage and KLF2, KLF3, KLF4, KLF5, KLF6, KLF7, KLF8, KLF9, KLF10, KLF11, KLF12, KLF13 and KLF15 expression were positive associated with ccRCC prognosis. Multivariate Cox proportional hazard regression analysis, based on the sixteen positive factors, revealed that age, grade, stage, KLF2 and KLF11 were independent factors for ccRCC prognosis (Table II). K-M survival curves of KLF2 and KLF11 (Fig. 1C) showed that patients with ccRCC who had low KLF2 and KLF11

Table II. Univariate and multivariate Cox risk ratio analysis of KLF gene expression and overall survival in patients with kidney renal clear cell carcinoma with The Cancer Genome Atlas data.

Characteristic	Univariate Cox			Multivariate Cox		
	HR	95% CI	P-value	HR	95% CI	P-value
Age	1.027	1.015-1.040	2.42×10^{-5}	1.023	1.009-1.037	0.001326
Sex	0.959	0.702-1.310	7.91×10^{-1}	-	-	-
Grade	2.638	1.872-3.718	3.04×10^{-8}	1.485	1.013-2.176	0.042861
Stage	3.733	2.715-5.132	5.09×10^{-16}	2.874	2.033-4.063	0.000229×10^{-5}
KLF2	0.703	0.615-0.804	2.39×10^{-7}	0.769	0.633-0.934	0.008103
KLF3	0.638	0.522-0.780	1.11×10^{-5}	1.405	0.820-2.407	0.216050
KLF4	0.728	0.641-0.826	8.71×10^{-7}	0.992	0.787-1.251	0.947531
KLF5	0.747	0.641-0.870	1.86×10^{-4}	0.854	0.713-1.024	0.088489
KLF6	0.681	0.594-0.782	4.45×10^{-8}	0.889	0.678-1.165	0.393358
KLF7	0.692	0.590-0.813	6.99×10^{-6}	1.381	0.904-2.110	0.135895
KLF8	0.843	0.714-0.996	4.48×10^{-2}	1.096	0.858-1.400	0.462576
KLF9	0.639	0.555-0.737	6.53×10^{-10}	0.926	0.646-1.328	0.676057
KLF10	0.756	0.663-0.863	3.24×10^{-5}	1.272	0.960-1.685	0.094032
KLF11	0.666	0.572-0.775	1.51×10^{-7}	0.594	0.366-0.964	0.035164
KLF12	0.622	0.521-0.742	1.44×10^{-7}	0.895	0.546-1.467	0.660072
KLF13	0.654	0.556-0.768	2.58×10^{-7}	0.917	0.645-1.303	0.629127
KLF15	0.751	0.664-0.849	4.73×10^{-6}	0.864	0.729-1.023	0.090373
KLF16	1.056	0.848-1.314	6.28×10^{-1}	-	-	-

CI, Confidence interval; HR, hazard ratio; KLF, Krüppel-like factor.

Table III. Multivariate Cox regression analysis.

Factor	coef	exp(coef)	se(coef)	Z-score	P-value
Age	0.025587	1.025917	0.006851	3.735	0.000188
Grade 3 + 4	0.406461	1.501494	0.188450	2.157	0.031016
Stage III + IV	1.088888	2.970967	0.170346	6.392	0.000164×10^{-6}
KLF2	-0.213400	0.807830	0.085902	-2.484	0.012982
KLF11	-0.197940	0.820422	0.091603	-2.161	0.030709

coef, co-efficient; exp (coef), expectation of co-ef; se (co-ef), standard error of co-ef.

expression had a lower survival probability. It suggests that the expression of KLF2 and KLF11 were associated with poor prognosis of ccRCC.

Prognostic models to assess the impact of KLFs and clinical characteristics on the prognosis of ccRCC. KLF2 and KLF11, which were screened from the multiple Cox regression analysis, were used to construct a predictive model. To investigate their effect on ccRCC prognosis, risk score was calculated as follows (Fig. 2A; Table III). Next, based on the median risk score, patients with ccRCC were divided into low- and high-risk groups (Fig. 2B). Heat map analysis was performed for the gene expression levels in the high and low-risk groups (Fig. 2E). K-M curve showed that patients in the high-risk group had worse survival than patients in

the low-risk group (Fig. 2C). In addition, the area under the ROC curve of risk score model was 0.780, indicating that it had an average diagnostic performance, as previously described (39) (Fig. 2D). These findings suggested that expression levels of KLF2 and KLF11 may be an independent predictor of ccRCC prognosis, according to the results of multivariate Cox regression analysis and prognostic predictive model. KLF2 and KLF11 were independent prognostic factors in ccRCC.

KLF2 overexpression inhibits cell migration of ccRCC. To validate the effect of KLFs on ccRCC cell lines, the expression of KLF2 and KLF11 in different ccRCC cell lines was examined using RT-qPCR and western blotting. KLF2 had lower expression in 786-O and 769-P cells than in HK-2
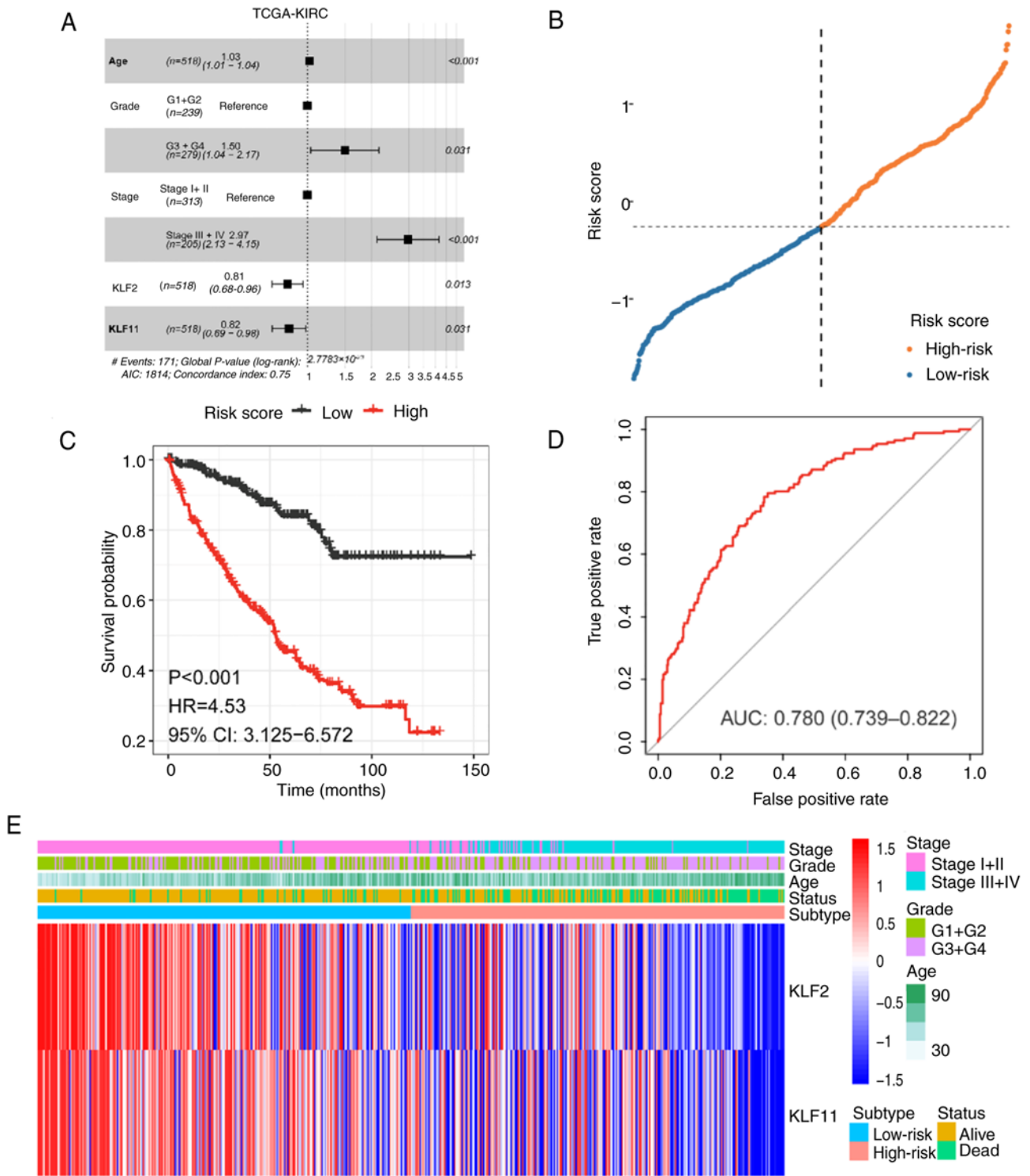
Figure 2. Prognostic role of KLF2 in ccRCC. (A) Hazard ratio of high- and low-risk groups. (B) Risk curve of each patient was categorized by risk score. (C) Kaplan-Meier curve analysis of patients with ccRCC. (D) AUC of the receiver operating characteristics curve plot was 0.780 for assessing accuracy of the prediction model. (E) Differential expression of KLF2 level in two groups as represented by heat map plots. KLF, Krüppel-like factor; ccRCC, clear cell renal cell carcinoma; AUC, area under the curve; TCGA-KIRC, The Cancer Genome Atlas-kidney renal clear cell carcinoma.

cells (Fig. 3A and B). Since KLF11 exhibit low expression in ccRCC (40), KLF2 was selected for further validation. To confirm the role of KLF2 in ccRCC migration, KLF2 plasmid was constructed and transfected into 769-P and 786-O cells for KLF2 overexpression (Fig. 3C). In the wound healing assay, the scratch width in the PCDH-CMV-KLF2 group was notably wider than in the control (Fig. 3D and E). These

findings suggested that increased expression of KLF2 impaired the cell migration. To validate the function of KLF2 in ccRCC, KLF2 expression was detected using a commercially available ccRCC TMA. IHC was performed on ccRCC clinical samples (Table IV) and the results indicated that the KLF2 protein level was significantly lower in stage II-III tissue compared with stage I tissue (Fig. 3F and G). These findings were
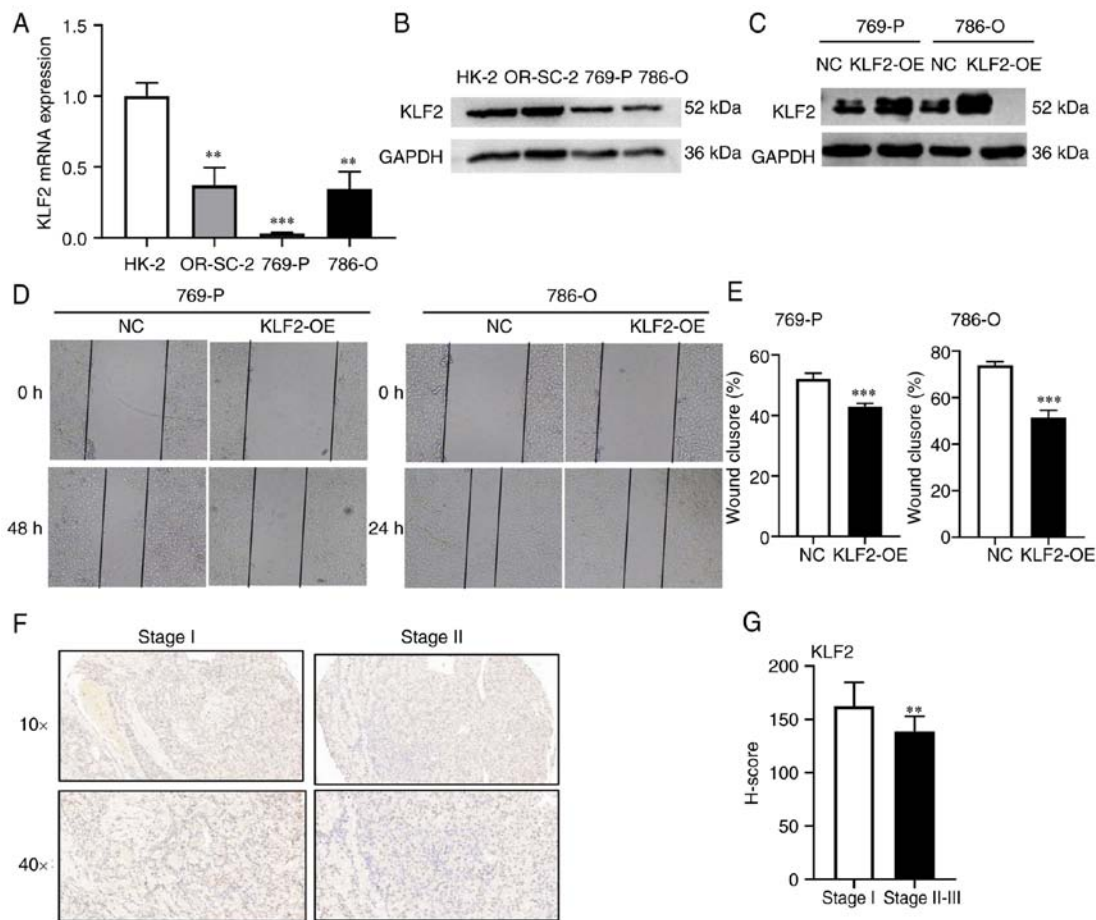
Figure 3. KLF2 inhibits ccRCC migration *in vitro* and KLF2 protein expression is decreased in high pathological grade tissue (II + III). (A) Expression of KLF2 mRNA in ccRCC and normal HK-2 cells. (B) Western blotting was used for assessment of KLF2 protein levels in ccRCC and normal HK-2 cells. (C) Western blotting assessment of KLF2 OE in 769-P and 786-O cells. (D) Migration of 769-P and 786-O cells after wounding (magnification, x40). (E) compared with NC. (F) Immunohistochemistry and (G) analysis of the KLF2 expression in ccRCC tissue (n=20). **$P<0.01$ vs. stage I and ***$P<0.001$ vs. NC. KLF, Krüppel-like factor; ccRCC, clear cell renal cell carcinoma; NC, negative control; OE, overexpression.

Table IV. Clinical characteristics of 20 patients with clear cell renal cell carcinoma.

Characteristic	n (%)
Sex	
Male	15 (75)
Female	5 (25)
Age, years	
≤55	8 (40)
>55	12 (60)
Tumor grade	
I	4 (20)
II + III	16 (80)
TNM stage	
T1 + T2	20 (100)
T3 + T4	0 (0)
Pt stage	
T1 + T2	20 (100)
T3 + T4	0 (0)
pM stage	
M0	20 (100)
M1	0 (0)

consistent with the aforementioned results of bioinformatics analysis. KLF2 was lowly expressed in cells and tissues, which overexpression of kLF2 inhibited cell migration.

KLF2 promoter methylation alterations. Examination of TCGA database using cBioPortal revealed that no genetic variations (data not shown) or methylation affected survival rate of patients with ccRCC. KLF2 exhibited 10 methylation sites (Table V). Univariate Cox analysis identified 8 candidate methylation sites for KLF2 (CG03725130, CG03725130, CG05906166, CG10819847, CG15496085, CG18473733, CG25266327 and CG26842024). Correlation analysis found significant differences between candidate methylation sites and expression of the KLF2 gene was significantly associated with candidate methylation sites (Fig. 4A). This implied that differences in KLF2 gene expression were associated with methylation. Based on this analysis, it was concluded that low expression of KLF2 was associated with poor survival and methylation. Therefore, KLF2 expression levels were detected after treatment of 769-P and 786-O cells with 5-AZA-CdR (a DNA methyltransferase inhibitor). The results showed that KLF2 protein expression increased after treatment (Fig. 4B and C). Overall, KLF2 expression levels are associated with poor prognosis, and DNA methylation may be involved.

Table V. Univariate analysis of KLF2 methylation sites.

CpG	HR	95% CI	P-value
KLF2-Body-Island-cg02668248	1.409	0.873-2.275	0.160
KLF2-TSS200-Island-cg03725130	0.332	0.190-0.578	<0.001
KLF2-Body-Island-cg04324758	3.252	1.740-6.079	<0.001
KLF2-Body-Island-cg05906166	8.040	3.263-19.808	<0.001
KLF2-TSS1500-Island-cg10819847	0.416	0.233-0.744	0.003
KLF2-TSS1500-Island-cg15496085	2.130	1.213-3.740	0.008
KLF2-Body-Island-cg18473733	1.687	1.004-2.836	0.048
KLF2-TSS1500-N_Shore-cg22247553	0.765	0.474-1.234	0.273
KLF2-5'UTR-Island-cg25266327	0.488	0.298-0.798	0.004
KLF2-Body-Island-cg26842024	2.179	1.438-3.304	<0.001

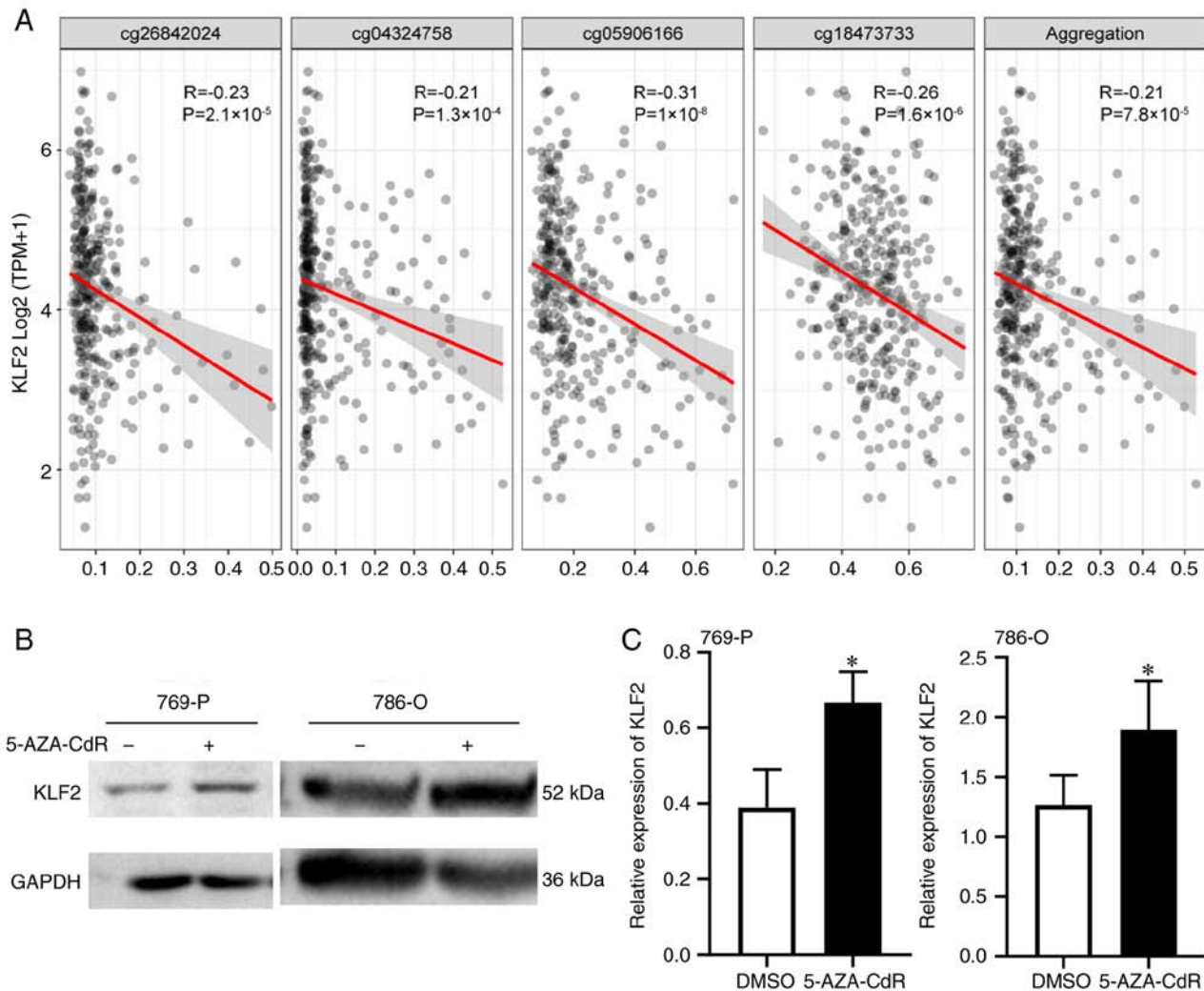CI, confidence interval; HR, hazard ratio; KLF, Krüppel-like factor; 5'UTR, 5' untranslated region.

Figure 4. Changes in KLF2 expression in clear cell renal cell carcinoma cell lines induced by the DNA methyltransferase inhibitor 5-AZA-CdR. (A) Correlation between KLF2 and methylation site. (B) Western blot assessment and (C) analysis of KLF2 protein expression in 769-P and 786-O cells following treatment with 5-AZA-CdR. *P<0.05 vs. DMSO group. KLF, Krüppel-like factor; 5-AZA-CdR, 5-aza-2'-deoxycytidine; TPM, transcripts per million.

Identify different pathway enrichment between high and low risk groups. GSVA enrichment analysis was used to determine the underlying mechanisms in the high- and low-risk groups.

This analysis revealed that the high-risk group was primarily enriched in 'E2F targets', 'allograft rejection' and 'EMT' (Fig. 5C). The Venn diagram identified co-negative regulation
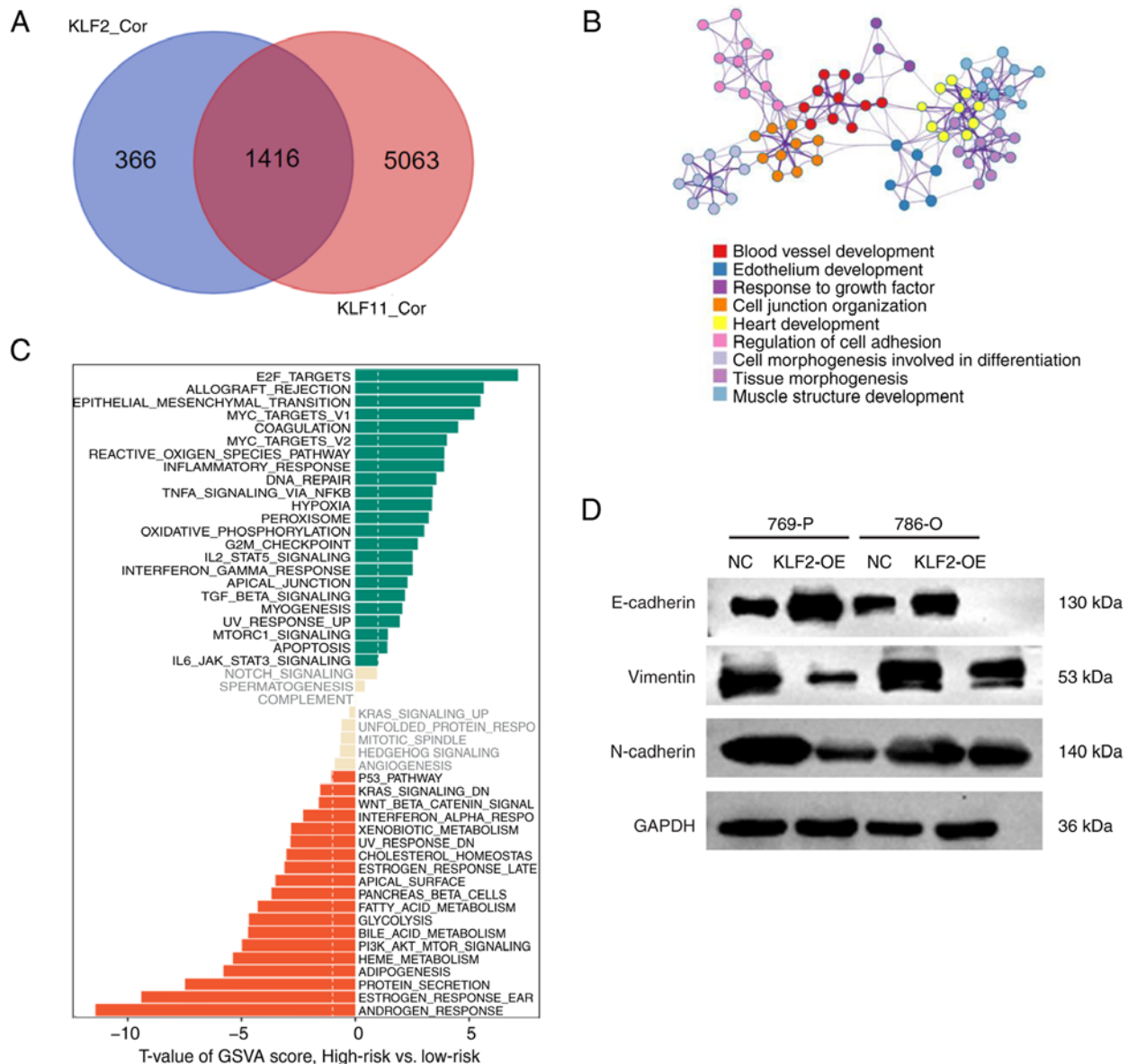
Figure 5. Venn plot and metascape enrichment of co-negative correlation between KLF2 and KLF11 genes. (A) Venn diagram showed co-negative regulation of KLF2 and KLF11. (B) Enriched GO items based on Venn diagram where different colors represent different GO biological processes. (C) Pathway enrichment analysis between high- and low-risk groups using GSVA. (D) Change in epithelial-mesenchymal transition-associated protein following KLF2 OE in 769-P and 786-O cells. GO, Gene Ontology; KLF, Krüppel-like factor; OE, overexpression; GSVA, Gene Set Variation Analysis.

of KLF2 and KLF11 for 1,416 co-regulated genes, which means these genes had highly correlated expression with both KLF2 and KLF11 (Fig. 5A). GO analysis of co-regulated genes demonstrated enrichment in 'regulation of cell adhesion' and 'cell junction organization' (Fig. 5B). Western blot analysis detected changes in expression of proteins involved in the EMT process. The level of E-cadherin was significantly downregulated, whereas the levels of N-cadherin and vimentin were increased following overexpression of KLF2 in 76P-P and 786-O cells (Fig. 5D). These findings suggested that the expression levels of KLF2 associated with EMT proteins.

Discussion

KLF family members are zinc-finger proteins that bind to DNA transcription regions, thus serving a vital role in transcriptional regulation (41). The involvement of KLFs in tumor progression has been widely reported (42-44). In the present study, gene expression levels and clinical factors were integrated to assess the prognostic value of KLFs. A prognostic model consisting of KLF2, KLF11, age, stage and grade was constructed from a TCGA cohort. The results showed that KLF2 was an independent prognostic factor for ccRCC. KLF2 acts as a nuclear transcription factor in pathophysiological processes, including immune inflammation (45,46), angiogenesis (47) and osteoclastogenesis (48) and is lowly expressed in numerous types of cancer. For example, overexpression of KLF2 inhibits cell proliferation, migration and metastasis in pancreatic ductal adenocarcinoma (49). Xue *et al* (50) demonstrated that KLF2 was downregulated in clinical tissue samples and cell lines of prostate cancer and observed that migration and invasion of prostate cancer cells were inhibited

following over-expression of KLF2. Xu et al (51) showed that KLF2 affects proliferation and apoptosis of gastric cancer cells by regulating transcription and expression of cyclin-dependent kinase genes. These aforementioned studies indicated that KLF2 serves a key role in cancer development. In addition, previous studies have shown that KLF2 functions as a vascular protective factor in nephropathy (52) and ccRCC resistance (53). Several studies (53-55) have reported the role of KLF2 in ccRCC. Lu et al (54) showed that KLF2 suppresses cell migration and invasion via ferroptosis in metastatic ccRCC. However, a recent study showed that, compared with paraneoplastic tissue, KLF2 is highly expressed in non-metastatic ccRCC (55). Thus, KLF2 serves different roles in different progressive stages of ccRCC. Similar studies on KLF2 have been conducted in hepatocellular carcinoma (56,57). However, only a few studies have reported the function of KLF2 in ccRCC (53-55). Therefore, the role of KLF2 in ccRCC requires further investigation.

The present study found that KLF2 was significantly under expressed in ccRCC; this was correlated with a poor prognosis. In vitro experiments confirmed that overexpression of KLF2 inhibited migration in the 786-O and 769-P cell lines. The present results were consistent a previous study (54). However, the mechanism of KLF2 in ccRCC needs to be further investigated. The present study highlighted methylation as an important mechanism for regulating KLF2 expression. Treatment with 5-AZA-CdR, a DNA methyltransferase inhibitor commonly used to deoxygenate DNA, restored KLF2 expression in ccRCC cells. Gene methylation is associated with tumor genesis and KLF2 methylation has been demonstrated in non-small cell lung cancer (58). However, to the best of our knowledge, the present study is first to report methylation of KLF2 in ccRCC. Whether changes in KLF2 methylation occur in ccRCC tissue remains to be determined in future studies. In addition, the present study performed simple signaling pathways assessment, which showed that KLF2 and KLF11 may decrease 'cell adhesion' and 'cell junction organization'. GSVA analysis revealed that 'EMT' was enriched in the high-risk group. Cell adhesion and migration are preconditions for cancer metastasis and 90% of patients with cancer to disease due to cancer-associated metastasis (59). In line with this, the present study found that, following overexpression of KLF2 in 769-P cells and 786-O cells, expression of EMT-associated proteins was significantly inhibited. These findings suggested that KLF2 may be a potential biomarker for predicting ccRCC development and progression. However, further studies on the potential prognostic value of KLF2 in ccRCC are necessary.

In conclusion, the present study analyzed expression of KLF2 in multiple types of cancer and highlighted its role in the prognosis of ccRCC. A risk model of KLFs was constructed and KLF2 expression appeared to have a favorable prognostic value. These results indicated that the expression of KLF2 may predict the prognosis of patients with ccRCC. Furthermore, novel ccRCC prognostic indicators may improve early diagnosis and access to therapy and increase patient survival. Future studies should evaluate the synergistic effect of KLF genes for immunotherapy. Further studies may provide comprehensive insight into the potential association between KLFs and ccRCC prognosis.

Availability of data and materials

The datasets used and/or analyzed during the current study are available from the corresponding author on reasonable request.

Authors' contributions

FT, JZ, GP and JD contributed to the conception, design and interpretation of the study. FH and YR performed the experiments and wrote the manuscript. ZW, HZ, YL and MW were responsible for the tissue preservation collection, statistical analysis and bioinformatics analysis in preparation of figures and tables. FH and YR confirmed the authenticity of all raw data. All the authors participated in revision of the manuscript. All authors have read and approved the final manuscript.

Ethics approval and consent to participate

The present study was approved by the ethics committee of The Second Affiliated Hospital, School of Medicine, The Chinese University of Hong Kong and a waiver of informed consent was granted (approval no. 2022004).

Patient consent for publication

Not applicable.

Competing interests

The authors declare that they have no competing interests.

References

1. Cohen HT and McGovern FJ: Renal-cell carcinoma. N Engl J Med 353: 2477-2490, 2005.
2. Mehdi A and Riazalhosseini Y: Epigenome aberrations: Emerging driving factors of the clear renal cell carcinoma. Int J Mol Sci 18: 1774, 2017.
3. Linehan WM and Ricketts CJ: The cancer genome atlas of renal cell carcinoma: Findings and clinical implications. Nat Rev Urol 16: 539-552, 2019.
4. Lucarelli G, Loizzo D, Franzin R, Battaglia S, Ferro M, Cantiello F, Castellano G, Bettocchi C, Ditonno P and Batting M: Metabolomic insights into pathophysiological mechanisms and biomarker discovery in clear cell renal cell carcinoma. Expert Rev Mol Diagn 19: 397-407, 2019.
5. Allen A, Gau D, Francoeur P, Sturm J, Wand Y, Martin R, Maranchie J, Duensing A, Kaczorowski A, Duensing S, et al: Actin-binding protein profilin1 promotes aggressiveness of clear-cell renal cell carcinoma cells. J Bio Chem 295: 15636-15649, 2020.

6. Wang Q, Zhang H, Chen Q, Wan Z, Gao X and Qian W: Identification of METTL14 in kidney renal clear cell carcinoma using bioinformatics analysis. Dis Markers 2019: 5648783, 2019.
7. Boustany J, Abdessater M, Hachem CE, Khoury ZE, Khoury WE and Khoury RE: Recurrent metastatic clear cell renal carcinoma with sarcomatoid dedifferentiation treated with surgery and Cabozantinib. Oncotarget 11: 1922-1928, 2020.
8. Cakici MC, Kır G, Akalın MK and Yıldırım A: Clear cell renal cell carcinoma with osseous metaplasia: Two extremely rare cases and review of the literature. Arch Esp Uro 73: 651-654, 2020 (In English, Spanish).
9. Zhao J and Eyzaguirre E: Clear cell papillary renal cell carcinoma. Arch Pathol Lab Med 143: 1154-1158, 2019.
10. Aeppli S, Eboulet EI, Eisen T, Escudier B, Fischer S, Larkin J, Gruenwald V, McDermott D, Oldenburg J, Omlin A, et al: Impact of COVID-19 pandemic on treatment patterns in metastatic clear cell renal cell carcinoma. ESMO Open 5 (Suppl 3): e000852, 2020.
11. Bersanelli M, Brunelli M, Gnetti L, Maestroni U and Buti S: Pazopanib as a possible option for the treatment of metastatic non-clear cell renal carcinoma patients: A systematic review. Ther Adv Med Oncol 12: 1758835920915303, 2020.
12. Rajandram R, Perumal K and Yap NY: Prognostic biomarkers in renal cell carcinoma: Is there a relationship with obesity? Transl Androl Urol 8 (Suppl 2): S138-S146, 2019.
13. Oates AC, Pratt SJ, Vail B, Yan YI, Ho RK, Johnson SL, Postlethwait JH and Zon LI: The zebrafish klf gene family. Blood 98: 1792-1801, 2001.
14. Moore DL, Blackmore MG, Hu Y, Kaestner KH, Bixby JL, Lemmon VP and Goldberg JL: KLF family members regulate intrinsic axon regeneration ability. Science 326: 298-301, 2009.
15. Chen Z, Lei T, Chen X, Zhang J, Yu A, Long Q, Long H, Jin D, Gan L and Yang Z: Porcine KLF gene family: Structure, mapping, and phylogenetic analysis. Genomics 95: 111-119, 2010.
16. Miller IJ and Bieker JJ: A novel, erythroid cell-specific murine transcription factor that binds to the CACCC element and is related to the Krüppel family of nuclear proteins. Mol Cell Biol 13: 2776-2786, 1993.
17. Ali A, Zhang P, Liangfang Y, Wenshe S, Wang H, Lin X, Dai Y, Feng XH, Moses R, Wang D, et al: KLF17 empowers TGF-β/Smad signaling by targeting Smad3-dependent pathway to suppress tumor growth and metastasis during cancer progression. Cell Death Dis 6: e1681, 2015.
18. Reidling JC and Said HM: Regulation of the human biotin transporter hSMVT promoter by KLF-4 and AP-2: Confirmation of promoter activity in vivo. Am J Physiol Cell physiol 292: C1305-C1312, 2007.
19. Saifudeen Z, Dipp S, Fan H and El-Dahr SS: Combinatorial control of the bradykinin B2 receptor promoter by p53, CREB, KLF-4, and CBP: Implications for terminal nephron differentiation. Am J Physiol Renal Physiol 288: F899-F909, 2005.
20. Seiler K, Soroush Noghabi M, Karjalainen K, Hummel M, Melchers F and Tsuneto M: Induced pluripotent stem cells expressing elevated levels of sox-2, oct-4, and klf-4 are severely reduced in their differentiation from mesodermal to hematopoietic progenitor cells. Stem Cells Dev 20: 1131-1142, 2011.
21. Shao M, Ge GZ, Liu WJ, Xiao J, Xia HJ, Fan Y, Zhao F, He BL and Chen C: Characterization and phylogenetic analysis of Krüppel-like transcription factor (KLF) gene family in tree shrews (Tupaia belangeri chinensis). Oncotarget 8: 16325-16339, 2017.
22. Shimeld SM: C2H2 zinc finger genes of the Gli, Zic, KLF, SP, Wilms' tumour, Huckebein, Snail, Ovo, Spalt, Odd, Blimp-1, Fez and related gene families from Branchiostoma floridae. Dev Genes Evol 218: 639-649, 2008.
23. Sun Y, Li Y, Wang M, Yue M, Bai L, Bian J, Hao W, Sun J, Zhang S and Liu H: Increased AT$_2$R expression is induced by AT$_1$R autoantibody via two axes, Klf-5/IRF-1 and circErbB4/miR-29a-5p, to promote VSMC migration. Cell Death Dis 11: 432, 2020.
24. Sunadome K, Yamamoto T, Ebisuya M, Kondoh K, Sehara-Fujisawa A and Nishida E: ERK5 regulates muscle cell fusion through Klf transcription factors. Dev Cell 20: 192-205, 2011.
25. Suske G, Bruford E and Philipsen S: Mammalian SP/KLF transcription factors: Bring in the family. Genomics 85: 551-556, 2005.
26. Fisch S, Gray S, Heymans S, Halder SM, Wang B, Pfister O, Cui L, Kumar A, Lin Z, Sen-Banerjee S, et al: Kruppel-like factor 15 is a regulator of cardiomyocyte hypertrophy. Pro Natl Acad Sci USA 104: 7074-7079, 2007.

27. Matsumoto N, Kubo A, Liu H, Akita K, Laub F, Ramirez F, Keller G and Friedman SL: Developmental regulation of yolk sac hematopoiesis by Kruppel-like factor 6. Blood 107: 1357-1365, 2006.
28. Nuez B, Michalovich D, Bygrave A, Ploemacher R and Grosveld F: Defective haematopoiesis in fetal liver resulting from inactivation of the EKLF gene. Nature 375: 316-318, 1995.
29. Wani MA, Means RT and Lingrel JB: Loss of LKLF function results in embryonic lethality in mice. Transgenic Res 7: 229-238, 1998.
30. Shindo T, Manabe I, Fukushima Y, Tobe K, Aizawa K, Miyamoto S, Kawai-Kowase K, Moriyama N, Imai Y, Kawakami H, et al: Krüppel-like zinc-finger transcription factor KLF5/BTEB2 is a target for angiotensin II signaling and an essential regulator of cardiovascular remodeling. Nat Med 8: 856-863, 2002.
31. Han M, Wang Y, Guo G, Li L, Dou D, Ge X, Lv P, Wang F and Gu Y: microRNA-30d mediated breast cancer invasion, migration, and EMT by targeting KLF11 and activating STAT3 pathway. J Cell Biochem 119: 8138-8145, 2018.
32. Wang X, Li X, Huang C, Li L, Qu H, Yu X, Ni H and Cui Q: Kruppel-like factor 4 (KLF-4) inhibits the epithelial-to-mesenchymal transition and proliferation of human endometrial carcinoma cells. Gynecol Endocrinol 32: 772-776, 2016.
33. Meng J, Lu X, Zhou Y, Zhang M, Gao L, Gao S, Yan F and Liang C: Characterization of the prognostic values and response to immunotherapy/chemotherapy of Krüppel-like factors in prostate cancer. J Cell Mol Med 24: 5797-5810, 2020.
34. Wen Y, Lu X, Ren J, Privratsky JR, Yang B, Rudemiller NP, Zhang J, Griffiths R, Jain MK, Nedospasov SA, et al: KLF4 in macrophages attenuates TNFα-mediated kidney injury and fibrosis. J Am Soc Nephrol 30: 1925-1938, 2019.
35. Liang K, Liu T, Chu N, Kang J, Zhang R, Yu Y, Li D and Li D: KLF8 is required for bladder cancer cell proliferation and migration. Biotechnol Appl Biochem 62: 628-633, 2015.
36. Livak KJ and Schmittgen TD: Analysis of relative gene expression data using real-time quantitative PCR and the 2(-Delta Delta C(T)) method. Methods 25: 402-408, 2001.
37. Maclean A, Bunni E, Makrydima S, Withington A, Kamal AM, Valentijn AJ and Hapangama DK: Fallopian tube epithelial cells express androgen receptor and have a distinct hormonal responsiveness when compared with endometrial epithelium. Hum Reprod 35: 2097-2106, 2020.
38. Dogan S, Vasudevaraja V, Xu B, Serrano J, Ptashkin RN, Jung HJ, Chiang S, Jungbluth AA, Cohen MA, Ganly I, et al: DNA methylation-based classification of sinonasal undifferentiated carcinoma. Mod Pathol 32: 1447-1459, 2019.
39. Yu J, Mao W, Sun S, Hu Q, Wang C, Xu Z, Liu R, Chen S, Xu B and Chen M: Identification of an m6A-related lncRNA signature for predicting the prognosis in patients with kidney renal clear cell carcinoma. Front Oncol 11: 663263, 2021.
40. Xi Z, Zhang R, Zhang F, Ma S and Feng T: KLF11 expression predicts poor prognosis in glioma patients. Int J Gen Med 14: 2923-2929, 2021.
41. Dai X, Ren T, Zhang Y and Nan N: Methylation multiplicity and its clinical values in cancer. Expert Rev Mol Med 23: e2, 2021.
42. Luo Y and Chen C: The roles and regulation of the KLF5 transcription factor in cancers. Cancer Sci 112: 2097-2117, 2021.
43. Marrero-Rodríguez D, la Cruz HA, Taniguchi-Ponciano K, Gomez-Virgilio L, Huerta-Padilla V, Ponce-Navarrete G, Andonegui-Elguera S, Jimenez-Vega F, Romero-Morelos P, Rodriguez-Esquivel M, et al: Krüppel like factors family expression in cervical cancer cells. Arch Med Res 48: 314-322, 2017.
44. Black AR, Black JD and Azizkhan-Clifford J: Sp1 and krüppel-like factor family of transcription factors in cell growth regulation and cancer. J Cell Physiol 188: 143-160, 2001.
45. Turpaev KT: Transcription factor KLF2 and its role in the regulation of inflammatory processes. Biochemistry (Mosc) 85: 54-67, 2020.
46. Jha P and Das H: KLF2 in regulation of NF-κB-mediated immune cell function and inflammation. Int J Mol Sci 18: 2383, 2017.
47. Novodvorsky P and Chico TJ: The role of the transcription factor KLF2 in vascular development and disease. Prog Mol Biol Transl Sci 124: 155-188, 2014.
48. Rolph D and Das H: Transcriptional regulation of osteoclastogenesis: The emerging role of KLF2. Front Immunol 11: 937, 2020.
49. Zhang D, Dai Y, Cai Y, Suo T, Liu H, Wang Y, Cheng Z and Liu H: KLF2 is downregulated in pancreatic ductal adenocarcinoma and inhibits the growth and migration of cancer cells. Tumor Biol 37: 3425-3431, 2016.

50. Xue P, Yan M, Wang K, Gu J, Zhong B and Tu C: Up-regulation of LINC00665 facilitates the malignant progression of prostate cancer by epigenetically silencing KLF2 through EZH2 and LSD1. Front Oncol 11: 639060, 2021.
51. Xu TP, Liu XX, Xia R, Yin L, Kong R, Chen WM, Huang MD and Shu YQ: SP1-induced upregulation of the long noncoding RNA TINCR regulates cell proliferation and apoptosis by affecting KLF2 mRNA stability in gastric cancer. Oncogene 34: 5648-5661, 2015.
52. Rane MJ, Zhao Y and Cai L: Krüppel-like factors (KLFs) in renal physiology and disease. EBioMedicine 40: 743-750, 2019.
53. Holland WS, Tepper CG, Pietri JE, Chinn DC, Gandara DR, Mack PC and Lara PN Jr: Evaluating rational non-cross-resistant combination therapy in advanced clear cell renal cell carcinoma: Combined mTOR and AKT inhibitor therapy. Cancer Chemother Pharmacol 69: 185-194, 2012.
54. Lu Y, Qin H, Jiang B, Lu W, Hao J, Cao W, Du L, Chen W, Zhao X and Guo H: KLF2 inhibits cancer cell migration and invasion by regulating ferroptosis through GPX4 in clear cell renal cell carcinoma. Cancer Lett 522: 1-13, 2021.
55. Li M, Zhang M, Chen M, Xiao J, Mu X, Peng J and Fan J: KLF2-induced circZKSCAN1 potentiates the tumorigenic properties of clear cell renal cell carcinoma by targeting the miR-1294/PIM1 axis. Cell Cycle: 1-15, 2022 (Epub ahead of print).
56. Zou K, Lu X, Ye K, Wang C, You T and Chen J: Krüppel-like factor 2 promotes cell proliferation in hepatocellular carcinoma through up-regulation of c-myc. Cancer Biol Ther 17: 20-26, 2016.
57. Jin L, He Y, Tang S and Huang S: LncRNA GHET1 predicts poor prognosis in hepatocellular carcinoma and promotes cell proliferation by silencing KLF2. J Cell Physiol 233: 4726-4734, 2018.
58. Jiang W, Xu X, Deng S, Luo J, Xu H, Wang C, Sun T, Lei G, Zhang F, Yang C, *et al*: Methylation of kruppel-like factor 2 (KLF2) associates with its expression and non-small cell lung cancer progression. Am J Transl Res 9: 2024-2037, 2017.
59. Zhang Y and Weinberg RA: Epithelial-to-mesenchymal transition in cancer: Complexity and opportunities. Front Med 12: 361-373, 2018.